

# Chemically Modified Alginate Bead Matrix for Efficient Adsorptive Recovery of Trypsin from Fresh Bovine Pancreas

## Pilar Aravena

Faculty of Biochemical and Pharmaceutical Sciences, Inst. of Biotechnological and Chemistry Processes, CONICET, National University of Rosario, Rosario, Argentina

## Maria Emilia Brassesco

Faculty of Biochemical and Pharmaceutical Sciences, Inst. of Biotechnological and Chemistry Processes, CONICET, National University of Rosario, Rosario, Argentina

## Barbara Bosio

Faculty of Biochemical and Pharmaceutical Sciences, Inst. of Biotechnological and Chemistry Processes, CONICET, National University of Rosario, Rosario, Argentina

## Guillermo Picó

Faculty of Biochemical and Pharmaceutical Sciences, Inst. of Biotechnological and Chemistry Processes, CONICET, National University of Rosario, Rosario, Argentina

## Nadia Voitovich Valetti

Faculty of Biochemical and Pharmaceutical Sciences, Inst. of Biotechnological and Chemistry Processes, CONICET, National University of Rosario, Rosario, Argentina

DOI 10.1002/btpr.2717

Published online 0, 2018 in Wiley Online Library (wileyonlinelibrary.com)

The adsorption of commercial trypsin (Try) onto epichlorohydrin cross-linked alginate–guar gum matrix has been studied at equilibrium in batch and in fixed bed column. Experiments were conducted to study the effect of ionic strength, temperature and to obtain a thermodynamic characterization of the adsorption process. The resulting adsorption isotherm fitted the Hill equation. Experimental breakthrough curve profiles were compared with the theoretical breakthrough profiles obtained from the mathematical model, bed depth service time. At pH 5.0, 1.0 g hydrated matrix adsorbed 480.0 milligram of Try per gram of dried bed. The desorption process showed 80% of Try recovery in 50 mM phosphate buffer, pH 7.00—500 mM NaCl—20% propylene glycol. The obtained results were applied to an adsorption/washing/desorption process with fresh pancreas homogenate yielded 20% of recovery and 5.7 purification factor of Try. The matrix remained functional until the fifth cycle of repeated batch enzyme adsorption. © 2018 American Institute of Chemical Engineers Biotechnol. Prog., 2018

*Keywords:* alginate, guar gum, polyelectrolytes, trypsin, adsorption, isotherms, breakthrough curves

## Introduction

From the classical work of Northrop and Kunitz in 1935<sup>1</sup> on the isolation and characterization of the pancreatic proteases, trypsin (Try), and chymotrypsin, different methods have been proposed to obtain these enzymes from its natural source: bovine fresh pancreas. The general way to isolate these enzymes is submerging the freshly collected pancreas in 0.25 N sulfuric acid. In a second step, a fractional precipitation using ammonium sulfate between 50 and 70% of saturation is used, where salt recovery and recycling are problematic. Another method proposes a previous activation of the pre-enzymes in a period of 4–12 h, with the purpose to isolate them with ionic exchange chromatography by a salt

gradient.<sup>2</sup> The problem with these methods is that they are expensive and generate a large amount of waste that negatively impacts the environment.

At present, one way to overcome this dilemma is by developing matrices with high affinity for these target proteins. In the last years, the use of natural polymers to obtain non-soluble matrices has received much attention in the downstream process of industrial enzymes,<sup>3–5</sup> as well as in the pharmaceutical field<sup>6,7</sup> for controlled drug delivery. The main reasons for this interest are their biocompatibility, cost-effectiveness, and discarding into the environment can be done without a negative impact.

Alginate (Alg) is a particularly attractive biopolymer with a wide range of applications in biomedicine, industrial food, and pharmaceutical fields. It has capacity to hold water and form gels and stable emulsions. Alg is a water-soluble linear polysaccharide composed of 1,4-linked  $\beta$ -D-mannuronic and

Correspondence concerning this article should be addressed to G. Picó at [pico@iprobyq-conicet.gob.ar](mailto:pico@iprobyq-conicet.gob.ar)

$\alpha$ -L-glucuronic acid residues, which are found in varying composition and sequence.<sup>8</sup> This polymer of natural origin has the advantage of being environmentally friendly as well as low in cost. The gelation of Alg can be carried out under an extremely mild environment using non-toxic reactants. Alg beads can be prepared by extruding a solution of sodium alginate as droplets into a divalent cation solution such as  $\text{Ca}^{2+}$  or  $\text{Ba}^{2+}$ .<sup>9</sup> A great number of papers show the transformation of Alg into a non-soluble matrix adding  $\text{Ca}^{2+}$  to the medium.<sup>9,10</sup> However, the working pH range of the matrix is limited, and when  $\text{Ca}^{2+}$  is lost by the matrix, the Alg- $\text{Ca}^{2+}$  complex is destroyed, making the Alg soluble.<sup>8</sup> The spherical matrix achieved in the drip step is permeable to small molecules and macromolecules, and they can interact because of the difference in their electrical charge. Therefore, this matrix can act as an ionic exchanger adsorbent for different molecules. However, the Alg matrices have a limited adsorption capacity, which depends in part of its porosity and the distance between the polymer chains. Previous works<sup>5,11</sup> have demonstrated that the incorporation of other nonelectrical-charged polysaccharide such as guar gum (GG) or xanthan gum induces an increase in the adsorption capacity of the matrix. GG is a non-ionic polysaccharide that is abundantly found in nature and has many properties desirable for drug delivery applications. GG is a water-soluble polysaccharide comprised high molecular weight (MW) polysaccharides composed of galactomannans consisting of a (1-4)-linked  $\beta$ -D-mannopyranose backbone with branch points from their 6-position linked to  $\alpha$ -D-galactose.<sup>12</sup> Alg-GG beads are not very stable, but the Alg-GG matrix cross-linked with epichlorohydrin (Epi) showed stability over a wide pH range and also in the presence of phosphate or  $\text{Ca}^{2+}$  chelator.<sup>4</sup>

In the area where our laboratory is located, meat industries are very important; therefore, great amounts of meat waste are produced. One of these products is the bovine pancreas. Therefore, the goal of this work was to analyze the adsorption capacity of Alg-GG matrix cross-linked with Epi for the serine protease, Try. The reason why this enzyme was chosen is because of its great use in different biotechnological processes. We have analyzed the kinetics behavior and adsorption isotherms in batch systems and also the adsorption and desorption of the commercial enzyme in fixed bed column. Finally, the results obtained with the commercial enzyme were applied in the purification of it from a natural source.

## Materials and Methods

### Chemical

Alginic acid sodium salt (Alg, 180947), GG (G4129), Epi (45340), N $\alpha$ -benzoyl-D,L-arginine-*p*-nitroanilide (BAPNA, B4875), and bovine trypsin (Try, T1426) were purchased from Sigma-Aldrich and used without further purification. All other reagents were also of analytical grade. The solutions were prepared with distilled water.

### Preparation of Alg-GG beads

Beads were formed by dropping Alg-GG solution (0.2% p/v and 0.5% p/v, respectively) through a syringe into a 0.1 M  $\text{CaCl}_2$  solution. Then, beads were cross-linking with Epi according to the method previously reported.<sup>5</sup> The matrix was finally resuspended in distilled water and equilibrated with the work buffer

before use. To check the intersection of matrices, we combine a certain amount of 0.1 M ethylenediaminetetraacetic acid (EDTA), which binds strongly to  $\text{Ca}^{2+}$ . EDTA detects the  $\text{Ca}^{2+}$  present in the sample, and if the cross-linking was not successful, the cation loss leads to the dissolution of the beads.

### Scanning electron microscopy

Scanning electron microscopy (SEM) micrograph of the cross-linked Alg-GG bead surface was performed using a scanning electron microscope FEI Quanta 650 FEG Environmental SEM with 3.00 kV voltage for secondary electron imaging. The macroparticles were previously treated immersing them in 2.5% glutaraldehyde diluted in 0.1 M sodium phosphate buffer pH 7.2 during 14 h. They were transferred three times for 10 min to 0.1 M phosphate buffer, pH 7.2. Then, they were dehydrated passing them two times during 5 min through ethanol solutions of 30%, 50%, 70%, 80%, 90%, 95%, and 100%. Finally, the beads were immersed in hexamethyldisilazane for 5 min, air dried at room temperature overnight, and mounted on copper tape.

### Fourier transforms infrared (FTIR) spectroscopy

IR studies were carried out in a Shimadzu Prestige 21, FTIR spectrometer, with an attenuated total reflectance accessory. The spectra were obtained with 40 scans per spectrum, in the wavenumber range of 4000–700  $\text{cm}^{-1}$  with a resolution of 4  $\text{cm}^{-1}$ . The samples were previously frozen at  $-50^\circ\text{C}$  and then lyophilized.

### Protein determination

Try activity was determined with the substrate BAPNA using a method modified by Gildberg and Overbo.<sup>13</sup> The reaction was followed by measuring the absorbance of the released reaction product, *p*-nitroanilide (using BAPNA as substrate in 100 mM buffer Tris-HCl pH 8.2.) which absorbs at 405 nm (molar absorptivity of 10,500  $\text{M}^{-1} \text{cm}^{-1}$ ). The assays were performed at constant temperature of 25  $^\circ\text{C}$ , and the activity was calculated from the slope of the initial linear portion of the absorbance vs. time curve. The concentration of protein in the medium was evaluated at 280 nm using a UV-VIS spectrophotometer. A calibration curve was performed using dilutions of a standard Try solution of 1 mg  $\text{mL}^{-1}$ .

### Determination of adsorption conditions

For adsorption of commercial Try, 3 mL of 25 mM citrate buffer with 0.4 mg  $\text{mL}^{-1}$  of Try were incubated with 100 mg of hydrated cross-linked Alg-GG matrix. Four pH values 4.0, 5.0, 6.0, and 7.0—and the following ionic strengths: NaCl 50 mM, 100 mM, and 200 mM—were assayed. The mixtures were stirred at 20 rpm until the adsorption equilibrium was reached. The free initial and final protein and the Try activity in the supernatant were determined. The amount of Try adsorbed was calculated from mass balance. The data were processed as milligram protein adsorbed per gram matrix. All measurements were carried out at 25  $^\circ\text{C}$ .

### Adsorption kinetics

To analyze the kinetic adsorption mechanism in a batch system, the amounts of Try adsorbed vs. time curves were determined and fitted with two mathematical models, namely pseudo-first and pseudo-second order. The adsorption kinetics was assayed at two temperatures and three different initial concentrations of enzyme. The mixtures were prepared with constant activity of Try in 25 mM citrate buffer pH 5.0 and stirring constantly at 20 rpm until the adsorption equilibrium was reached.

### Adsorption isotherms

Adsorption isotherms of Try were determined by equilibrating different concentrations of Try with 100 mg cross-linked Alg-GG beads at pH 5.0 and two different temperatures 25 °C and 8 °C. The mixtures were stirred until the adsorption equilibrium was reached, and the free initial and final protein concentration in the supernatant were determined.

### Thermodynamic evaluation

The thermodynamic state functions (free energy, enthalpic, and entropic changes) are important indicators when estimating the mechanism of the adsorption process. The standard Gibbs energy ( $\Delta G^\circ$ ), enthalpic ( $\Delta H^\circ$ , kJ mol<sup>-1</sup>), and entropic changes ( $\Delta S^\circ$ , J K mol<sup>-1</sup>) were estimated by applying the thermodynamic equations as follows:

$$\Delta G^\circ = \Delta H^\circ - T\Delta S^\circ \quad (1)$$

$$\ln K_0 = \frac{\Delta S^\circ}{R} - \frac{\Delta H^\circ}{RT} \quad (2)$$

where  $R$  is the universal gas constant ( $8.314 \times 10^{-3}$  kJ mol<sup>-1</sup> K<sup>-1</sup>),  $T$  is the absolute temperature (K), and  $K_0$  is the adsorption equilibrium constant of the enzyme between the adsorbed layer and the solution.

### Adsorption in column: breakthrough curves modeling

A continuous adsorption study was carried out making use of fixed bed column chromatography. In this process, a mass transfer occurs between two phases: the mobile phase, containing the solute, and the solid phase of the fixed bed constructed with the cross-linked Alg-GG matrix. The chromatography was performed in a glass column of 5 mm internal diameter  $\times$  100 mm height. A solution of known concentration of commercial Try was pumped at constant rate through the column. The elution procedure was performed using a Akta 100 (GE Healthcare, Uppsala, Sweden) equipped with a peristaltic pump and a UV detection for the protein concentration measurements. The data obtained were expressed as  $C/C_0$ —protein concentration in the eluate over total initial Try concentration in the inlet solution—vs. time.

### Data analysis

A nonlinear regression analysis was applied to estimate the isothermal and kinetic model parameters. Nonlinear regression was performed using a trial and error method with the help of

Sigma Plot v12 software. In the trial and error procedure, isothermal and kinetic parameters were estimated by maximizing the coefficient of determination ( $R^2$ ) (sum of squares) and minimizing the value of SS (least sum of squares). Both coefficients have been widely used to measure the fitting degree of the isothermal and kinetic model to adsorption data.<sup>14,15</sup>

### Evaluation of the performance of the purification process

Finally, the obtained results were applied to the purification of Try from freshly activated bovine pancreas homogenate.<sup>16</sup> The recovery and the purification factor were calculated, and aliquots of samples were analyzed by sodium dodecyl sulfate (SDS) polyacrylamide gel electrophoresis (PAGE). The running time was about 2 h with a constant intensity of 25 mA for the resolving gel. Proteins were stained with Coomassie brilliant blue.

## Results and Discussion

### Characterization of the matrix

The cross-linked Alg-GG bead was morphologically studied by SEM. The dried beads presented an irregular shape with a mean particle diameter of 1.0 mm (Figure 1A). At 50  $\mu$ m, the surface looks rough and porous in appearance (Figure 1B) with an increase in surface area making the molecules in the aqueous phase more suitable for a further adsorption process. Figure 2 shows the IR spectra of Alg-GG before and after cross-linking it with Epi. Alg-GG has a band of high intensity at 3443 cm<sup>-1</sup> which is because of the stretching of —OH bond in both polymers. The bands around 1633 and 1422 cm<sup>-1</sup> correspond to the asymmetric stretching of Alg-COO, whereas the bands between 800 and 1200 cm<sup>-1</sup> are associated to the stretching of C—C—O, C—OH, and C—O—C bonds, which are interacting between them in both polymers. The spectrum for cross-linked matrix shows a band at 1100 cm<sup>-1</sup> because of the epoxy group and the axial deformation of C—O—C.

### Batch adsorption studies

All batch adsorption experiments detailed below were conducted with commercial enzyme (Try) at constant temperature and stirring.

**Determination of Adsorption Conditions.** Because the interaction between the electrically charged bed and a protein is dependent on the pH and ionic strength of the medium, these variables were assayed, as shown in Figure 3. The pH value of 5.0 was suitable to adsorb Try, and the increasing concentration of NaCl decreases the adsorption yield; therefore, the next experiments were performed in a medium at pH 5.0 without adding NaCl. These results are consistent with an electrostatic interaction mechanism between Try and Alg-GG beads.

**Kinetic Studies.** The adsorption kinetics was assayed at two temperatures. In both cases, the adsorbed protein increases with contact time until it reaches a plateau as shown in Figure 4A. The point where the plateau begins is the equilibrium time required to achieve the maximum adsorption under these conditions. A rapid uptake and a short time in the

equilibrium establishment indicate the usefulness of the adsorbent in protein adsorption from a biomass solution. Available adsorption studies in literature reveal that the uptake of adsorbate species is fast at the initial stages of the contact period, and thereafter, it becomes slower near the equilibrium. Between these two stages, the rate of adsorption is nearly constant. This is because many vacant surface sites are available for adsorption during the initial stage, and after a lapse of time, the remaining vacant surface sites are difficult to be occupied because of repulsive forces between the solute molecules on the solid and bulk phases. Adsorption kinetics models are used to explain the adsorption mechanism and adsorption characteristics. To analyze the adsorption kinetics mechanism, the experimental data were fitted with two kinetics models, called pseudo-first and pseudo-second order as shown in Eqs. 3 and 4, respectively.

$$q_t = q_e(1 - e^{-k_1 t}) \quad (3)$$

$$q_t = \frac{k_2 q_e^2 t}{1 + k_2 q_e t} \quad (4)$$

where  $k_1$  and  $k_2$  are the first and second order kinetics constant, respectively and  $q_t$  and  $q_e$  are the amounts of Try adsorbed per gram of matrix in a time “ $t$ ” and at the equilibrium, respectively.<sup>17</sup> The parameters of the kinetic models and

the regression correlation coefficients ( $R^2$ ) are listed in Table 1. It can be concluded that the adsorption of Try onto Alg–GG matrix follows, at both temperatures, a pseudo-first-order kinetic. The adjustments to this model not only present the highest  $R^2$  and the lowest SS values, but also results in the same  $q_e$  values that are observed experimentally. This suggests that external mass transfer was the limiting step in Try adsorption onto Alg–GG beads.

**Isotherms Modeling.** We performed the isothermal adsorption at pH 5.0—optimal pH previously found—and we analyzed the temperature effect on the adsorption. By visual inspection of the experimental data (Figure 4B), a high adsorption of enzyme at low enzyme concentration can be seen. To optimize the design of an adsorption system, it is important to establish the most appropriate correlation for the equilibrium data. Various isotherm equations have been used to describe the isotherm curve.<sup>18</sup> To estimate the validity of the isotherm models with experimental data, two-parameter equations were used: Freundlich and Langmuir, and three-parameter equation: Hill model, as shown in Table 2.

The statistical analysis of the error function shows that the equation which has the best data fit for both temperatures assayed is the Hill model. Figure 4B shows this fit in the experimental data. This model assumes that the adsorption process is a cooperative phenomenon, where the ability of the ligand to bind at one binding site on the macromolecule is influenced by the presence or not of ligands bound to different binding sites on the same macromolecule.<sup>19</sup>

Table 3 shows how the Hill cooperatively coefficient increases with the increase in temperature, thus suggesting that temperature favors the separation of bed polysaccharides chain present in the bed, allowing the penetration of the Try molecules onto matrix, which is coincident with the increase of the  $K_D$  values. This can be because of the solvent loss from the matrix and to the decrease in the thickness of the boundary layer of water that surrounds the adsorbent. Besides, cooperative effect depends on different medium variables such as pH, and temperature changes. It can be seen that the cooperative effect is higher at 25 °C, which might indicate a modification in the adsorption mechanism with temperature variations.<sup>18</sup> The thermodynamic variable values calculated using Eqs. 2 and 3 yielded the following values:  $\Delta H^\circ = 37.7 \text{ kcal mol}^{-1}$  and  $\Delta S^\circ = 150 \text{ cal kmol}^{-1}$ . A positive  $\Delta H^\circ$  indicates that the adsorption process was endothermic consistent with the breakage of water–matrix interaction (water-hydroxyl bound by hydrogen bridge). Because the  $\Delta S^\circ$  was positive, this function contributes negatively to the  $\Delta G^\circ$  of adsorption; therefore, it can be considered adsorption as entropically driven.

**Protein Release from the Matrix.** Try elution from the matrix was carried out at 25 °C. After adsorption, the matrix loaded with the enzyme was washed with the working buffer until a negligible 280 nm absorbance measurement. For elution, the beads were incubated with six different medium—25 mM citrate buffer pH 7.0 and 25 mM Tris–HCl buffer pH 8.2, both with three increasing NaCl concentration solutions—and stirred for 1 h. Finally, the concentration of Try in the supernatant was measured. Because pH and ionic strength affect the adsorption, the effect of these variables was assayed.<sup>5,11</sup> We selected pH values that decrease the positive charge of Try thereby lowering the enzyme–matrix interaction. The results are shown

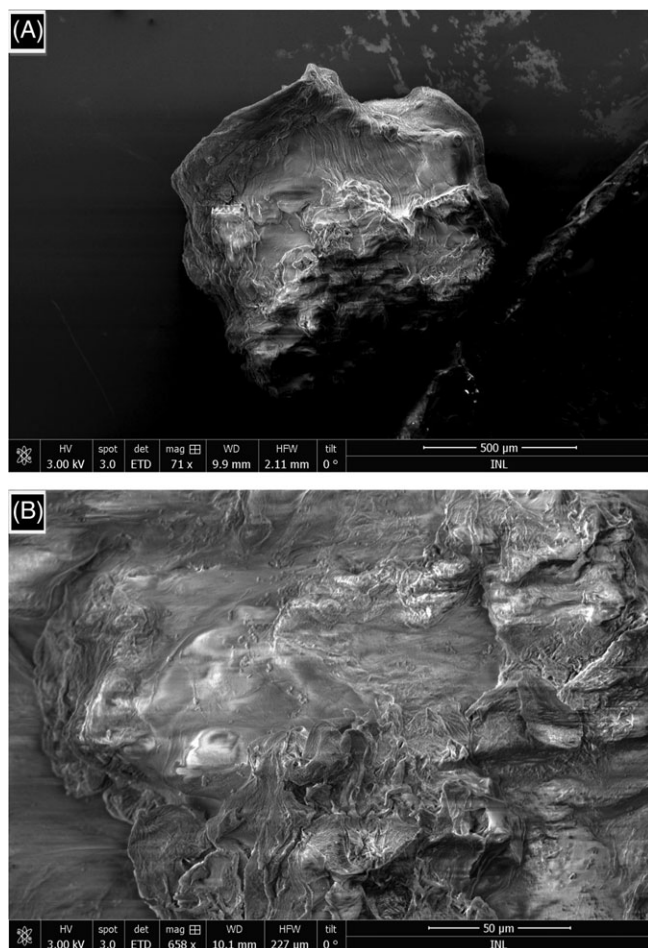


Figure 1. SEM of Alg–GG Epi cross-linked.

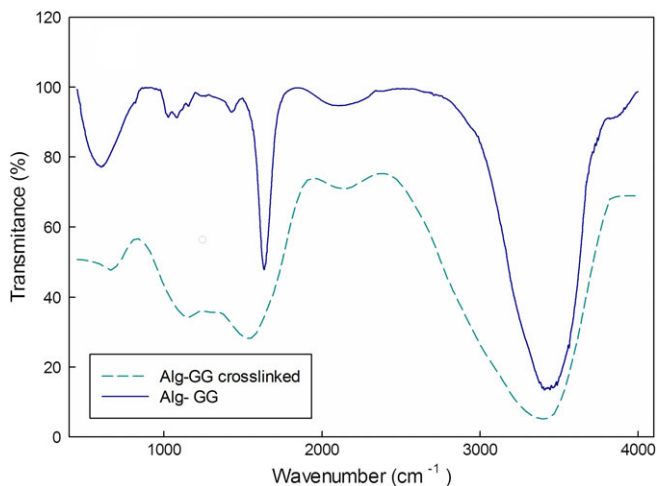


Figure 2. IR spectra of Alg-GG and Alg-GG Epi cross-linked.

in Table 4 as percent of Try eluted in relation to the Try amounts bound to the matrix in the adsorption step. It can be concluded that the change of pH from 7.0 to 8.2 and the presence of NaCl from 0 to 1.0 M did not produce the enzyme elution in a significant manner, where only a 40% of the enzyme was lost from the matrix. The presence of ammonium sulfate also did not induce an increase in the elution process; this salt was assayed because it is well known that has properties to help lose the protein bound to a matrix by hydrophobic forces. Propylene glycol has been used to induce the elution process of proteins bound to polysaccharides matrices such as phenyl Sepharose®. It has been postulated that this synthetic organic compound and other solutes, such as urea or dimethyl sulphoxide, decrease the water activity, inducing a water flow from the pore of the matrix to the exterior.<sup>20</sup> Therefore, according to Timasheff, a decrease in the pore radius produces a loss of the protein from its interior. Consequently, we induced the elution of the enzyme using propylene glycol at 20%. The observed recovery was, once again, low (around 30%). However, when a mixture of propylene glycol 20% and a variable NaCl concentration was used, the elution was significantly higher, showing a top value of 75% of Try eluted in the presence of 500 mM NaCl, higher salt concentration produced the inverse effect.

**Bed Regeneration.** Finally, any adsorbent is economically viable if it can be regenerated and reused in many operational cycles. For the reutilization study of the matrix, successive cycles of adsorption–washing–elution were carried out using the same matrix as adsorbent and an excess of protein. The concentration of recovered Try was determined in each step. The process was repeated several times in different days. It was found that the adsorption capacity of the matrix was not modified in this period (data not shown). However, in the fifth cycle, a loss of functionality was observed, with only 53% of enzyme recovery in desorption step.

#### Dynamic adsorption of Try: fixed bed and influence of operating parameters on its adsorption

Fixed bed column studies were carried out using a glass column of 5 mm internal diameter and 100 mm length. The Alg-GG matrix was packed in the column in the same buffer

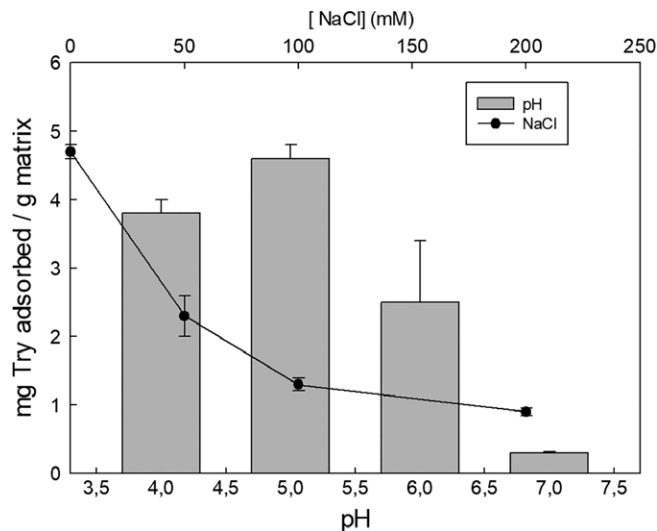


Figure 3. pH and NaCl effect on the Try adsorption onto Alg-GG matrix. Medium: citrate buffer 25 mM, temperature 25 °C.

used in the batch adsorption experiments (25 mM citrate buffer, pH 5.0), and the following experiments were performed:

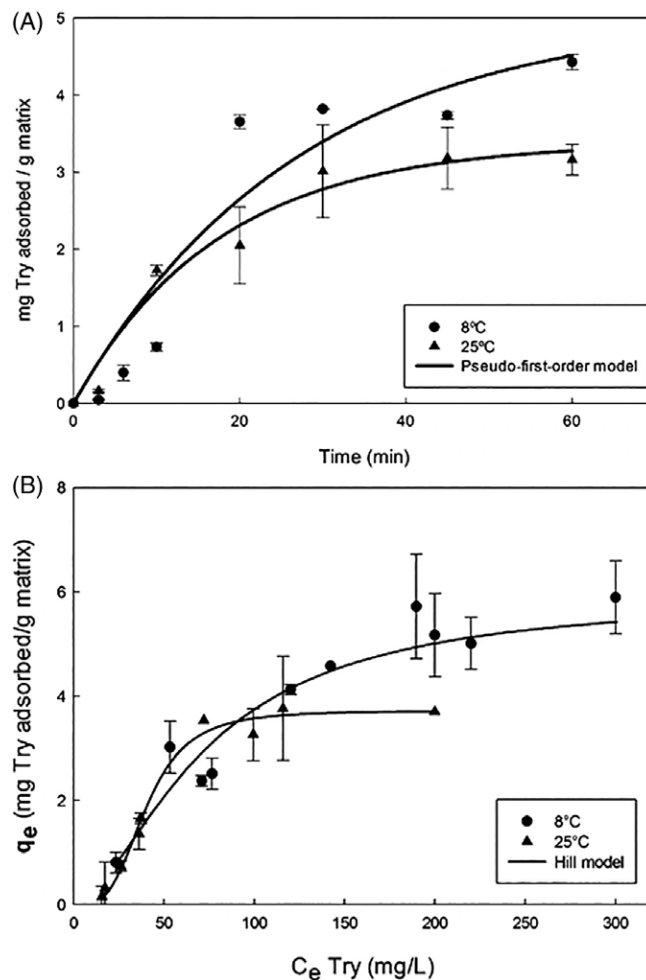


Figure 4. (A) Kinetic of Try adsorption onto Alg-GG matrices. Medium: citrate buffer 25 mM, pH 5.0. [Try]: 0.4 mg mL<sup>-1</sup>. (B) Adsorption isotherm of Try onto non-soluble Alg-GG beads. Medium: citrate buffer 25 mM, pH 5.0.

**Table 1. Kinetic Parameters for Try Adsorption onto Alg-GG Beads. [Try]: 0.4 mg mL<sup>-1</sup>. Medium: 25 mM Citrate Buffer, pH 5.0**

Model		8 °C	25 °C
Pseudo-first order	$q_e$ (mg g <sup>-1</sup> )	5.0 ± 1.0	3.4 ± 0.3
	$k_1$ (min <sup>-1</sup> )	(4 ± 2) × 10 <sup>-2</sup>	(6 ± 1) × 10 <sup>-2</sup>
	$R^2$	0.9015	0.9695
	SS	2.647	0.3401
Pseudo-second order	$q_e$ (mg g <sup>-1</sup> )	7.0 ± 1	5.0 ± 1
	$k_2$ (g mg <sup>-1</sup> min <sup>-1</sup> )	(3 ± 1) × 10 <sup>-3</sup>	(1.3 ± 0.1) × 10 <sup>-2</sup>
	$h$ (k <sub>2</sub> q <sub>e</sub> <sup>2</sup> ) (mg min <sup>-1</sup> g <sup>-1</sup> )	0.2 ± 0.1	0.23 ± 0.05
	$R^2$	0.8931	0.9623
	SS	2.874	0.4203

**Effect of Bed Height.** The effect of varying bed heights (3.0, 5.0, and 8.0 cm) on breakthrough curves at constant flow rate of 0.3 mL min<sup>-1</sup> and with injection protein volume of 0.5 mL ([Try] = 25 mg mL<sup>-1</sup>) was investigated, and the results are shown in Figure 5A. As the Try solution passes through the bed, the adsorption zone moves out of the column, and Try concentration starts increasing with time. This is known as breakthrough point. The time over which a Try concentration reaches a specific breakthrough concentration is called breakthrough time ( $t_b$ ).<sup>21</sup> The  $t_b$  for each curves was defined as the time when the concentration ( $C_0$ ) of Try reached 50% of the inlet concentration ( $C$ ). The results indicate that higher the bed height, more binding sites are available and higher the  $t_b$  value resulting in higher mass transfer zone.<sup>22</sup> Therefore, it is concluded that an increase in Try uptake in column with increasing bed heights is because of increase in the time of contact with the biosorbent.

**Effect of Flow Rate.** It was investigated by varying flow rate (0.2–0.4 mL min<sup>-1</sup>) at constant bed height (8.0 cm, selected based on previous results) and injection volume (0.5 mL, [Try] = 25 mg mL<sup>-1</sup>). The breakthrough curve of  $C_0/C$  vs. time with varying flow rate is depicted in Figure 5B. The results indicated that a decreasing in flow rate at a constant bed height increase the breakthrough time ( $t_b$ ).

**Effect of Try Injection Volume.** The variation of the protein injection volume (0.1, 0.5, and 1.0 mL, [Try] = 25 mg mL<sup>-1</sup>) on performance of breakthrough curves at constant bed height (8.0 cm) and flow rate of 0.3 mL min<sup>-1</sup> is given in Figure 5C. These curves show that as the initial concentration of Try increases, the time of breakthrough point also increases.

#### **Bed Depth Service Time (BDST) Model Applied to the Fixed Bed Column.**

The BDST model is based on surface reaction theory and provides information about efficiency of column operating under constant conditions.<sup>23</sup> This model can be used to obtain desired breakthrough curves. A plot of bed height ( $Z$ ) against time for 10–99% breakthrough at constant  $Q$  and  $C_0$  based on the BDST model was carried out (data not shown). The BDST model assumes that the rate of adsorption is controlled by the surface reaction between the adsorbate and the residual capacity of the adsorbent. This model is used to describe the initial part of the breakthrough curve, which

relates  $C/C_0$  to time,  $t$ , for a continuous-flow adsorbed column. Bohart and Adams equation has the following form:<sup>24</sup>

$$\ln\left(\frac{C_0}{C} - 1\right) = \ln\left[\exp\left(kN_0\frac{Z}{U}\right) - 1\right] - k_0C_0t \quad (8)$$

where  $C_0$  is the initial concentration of sorbate (mg dm<sup>-3</sup>),  $C$  is the desired concentration of sorbate at time  $t$  (mg dm<sup>-3</sup>),  $k$  is the sorption rate constant of the column (dm<sup>3</sup> min<sup>-1</sup> mg<sup>-1</sup>),  $Z$  is the length of the bed (cm),  $N_0$  is the adsorptive capacity of the adsorbent bed (mg dm<sup>-3</sup>), and  $U$  is the linear flow velocity of the feed to the bed (cm min<sup>-1</sup>). Hutchins linearized Eq. 8 to give:<sup>23</sup>

$$t = \frac{N_0}{C_0U}Z - \frac{1}{kC_0} \ln\left(\frac{C_0}{C} - 1\right) \quad (9)$$

Eq. 9 may be rewritten as:

$$t = aZ + b, \quad (10)$$

where

$$a = \frac{N_0}{C_0U} \quad (11)$$

and

$$b = \frac{1}{kC_0} \ln\left(\frac{C_0}{C} - 1\right) \quad (12)$$

The dynamic capacity of the bed can be evaluated from the slope  $a$  of the string line, and the rate constant,  $k$ , can be calculated from the intercept  $b$ . A linear relation between  $t$  and  $Z$  was obtained, according to Eqs. 11 and 12, the values of  $N_0$  and  $k$  were calculated at different ratio  $C/C_0$  (0.1–0.99), and they are presented in Table 5, together with the correlation coefficients ( $R^2 > 0.9304$ ) and smaller SS (less than 0.033). As the value of  $C/C_0$  increases, the rate constant and  $N_0$  also increase. The values of  $R^2$  and SS indicate the validity of the BDST model from the present system between 0.3 and 0.75  $C/C_0$ . According to the BDST

**Table 2. Equations for Isotherm Modeling**

Models	Formula	Parameters
Freundlich	$q_e = K_F C_e^{1/n}$ (5)	$K_F$ : Freundlich isotherm constant, $n$ : adsorption intensity
Langmuir	$q_e = \frac{Q_0 K_L C_e}{1 + K_L C_e}$ (6)	$K_L$ : Langmuir isotherm constant, $Q_0$ : monolayer coverage capacity
Hill	$q_e = \frac{Q_0 C_e^{n_H}}{K_H + C_e^{n_H}}$ (7)	$K_H$ : Hill constant, $n_H$ : cooperativity coefficient

In all models,  $q_e$  denotes the adsorbate adsorbed per gram of adsorbent at equilibrium and  $C_e$  is the equilibrium concentration of adsorbate.

**Table 3. Isotherms Parameter Values for Try Adsorption onto Alg-GG Matrix. Medium: 25 mM Citrate Buffer, pH 5.0**

Isotherm	Parameter	8 °C	25 °C
Langmuir	$Q_0$ (mg g <sup>-1</sup> )	4.0 ± 2.0	7.0 ± 2.0
	$K_L$ (L mg <sup>-1</sup> )	$(1.1 ± 0.3) × 10^{-2}$	$(8 ± 5) × 10^{-3}$
	$R^2$	0.8789	0.8668
	SS	3.071	2.434
Freundlich	$N$	2 ± 3	5 ± 1
	$K_F$ (L g <sup>-1</sup> )	0.34 ± 0.08	0.6 ± 0.2
	$R^2$	0.7544	0.7955
Hill	SCE	6.199	3.734
	$K_D$	72 ± 12	40 ± 3
	$Q_0$	5.9 ± 0.5	3.7 ± 0.2
	$n_H$	1.7 ± 0.5	3.5 ± 0.8
	$R^2$	0.9138	0.9850
	SS	2.175	0.2227

model, Try adsorption is governed by a complex mechanism involving more than one rate controlling step.<sup>25</sup> However, the mathematical model shows to be useful in the range of breakthrough curve.

**Use of the matrix to recover Try from a freshly homogenized pancreas**

Using the above determined conditions, both adsorption methods—batch and fixed bed—were assayed for study the recovery of Try from fresh bovine pancreas without previous treatment. In first instance, batch adsorption-desorption was studied, and we obtained a recovery of 15% with a purification factor of 2.0. In the way to increase the recovery, the adsorption-desorption process was carried out in fixed bed; 2.0 g of matrix was placed in a column of 5 mm diameter and 100 mm of height, equilibrated with the same buffer of adsorption, and 10.0 mL of homogenate was passed through the column with a rate of 0.3 mL min<sup>-1</sup>, then the column was washed with the same buffer of adsorption and the enzyme eluted with buffer pH 7.0—NaCl 500 mM—propylene glycol 20%. The recovery was around 20% with a purification factor 5.7.

Figure 6 shows a SDS-PAGE electrophoresis of the homogenate and the eluate. A significant number of proteins present in the homogenate (Lane 3) are absent in the elution solution (Lane 2). The adsorption showed to be no specific only for Try, because in the electrophoresis gel, three bands are observed. If the protein composition of the bovine pancreas<sup>26</sup> and the MW of the proteins present in higher proportion are taken into account, the bands obtained can be attributed to other pancreatic proteases

**Table 4. Percentage of Try Recovered Using Different Elution Medium. Try Adsorption was Preformatted at 25 °C and at 0.4 mg mL<sup>-1</sup> of Initial Enzyme Concentration**

Elution Medium	% Try Eluted
pH 7.00	11.3
pH 7.00—500 mM NaCl	25.4
pH 7.00—750 mM NaCl	32.9
pH 8.20	5.4
pH 8.20—500 mM NaCl	42.3
pH 8.20—1 M NaCl	33.6
(NH <sub>4</sub> ) <sub>2</sub> SO <sub>4</sub> 500 mM	23.5
pH 7.00—20% propylene glycol	32.3
pH 7.00—20% propylene glycol + 500 mM NaCl	76.0
pH 7.00—20% propylene glycol + 750 mM NaCl	65.9
pH 7.00—20% propylene glycol + 1 M NaCl	56.0

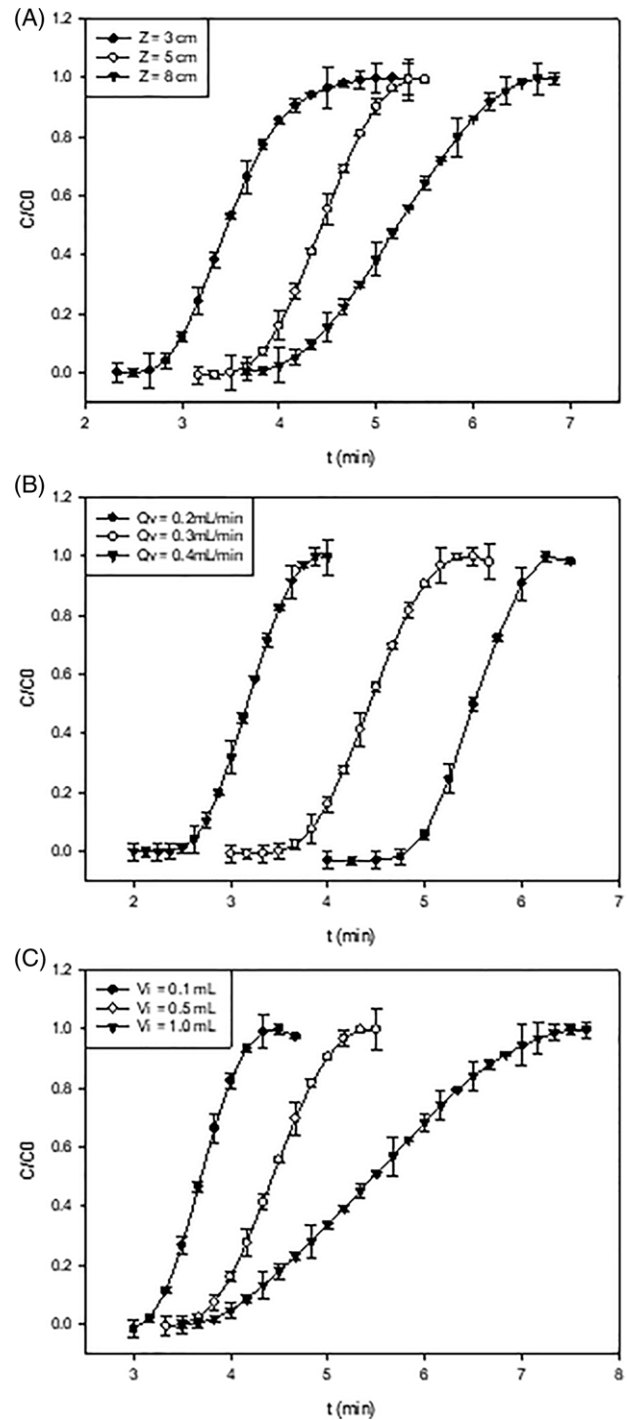


**Figure 5. Breakthrough curves from the Try adsorption onto Alg-GG bed at different variables: (A) bed height, (B) flow rate, and (C) Try injection volume. Medium: citrate buffer 25 mM, pH 5.0, temperature 25 °C.**

**Table 5. Adams-Bohart Parameters Under Different Conditions**

$C/C_0$	$k$ (L mg <sup>-1</sup> cm <sup>-1</sup> )	$N_0$ (mg L <sup>-1</sup> )	$R^2$	SS <sup>2</sup>
0.10	0.225	2.40	0.9642	0.033
0.30	0.258	2.53	0.9872	0.020
0.50	0.283	2.7	0.9897	0.015
0.75	0.317	2.76	0.9997	0.016
0.99	0.316	3.70	0.9304	0.135

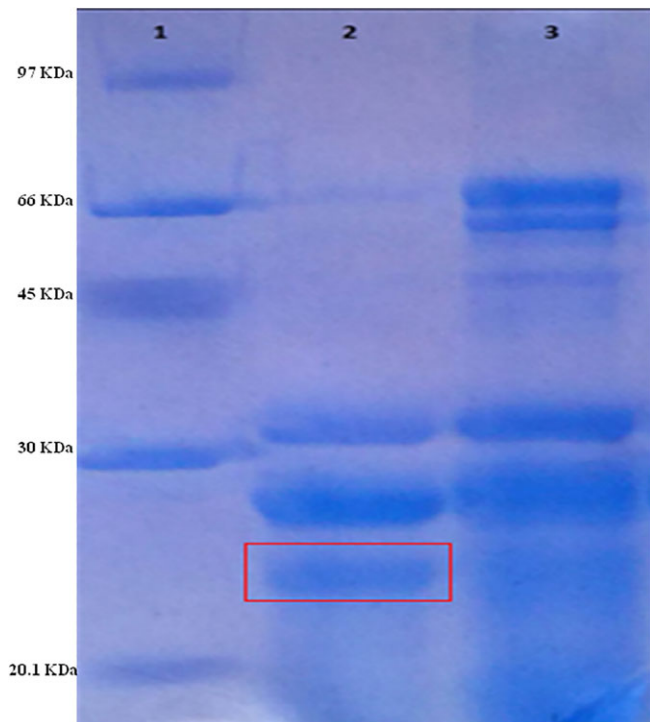


**Figure 6.** SDS-PAGE for the pancreas homogenate proteins: (1) molecular marker, (2) elution from the fixed bed, and (3) homogenate.

such as carboxypeptidase (34.5 kDa)<sup>27</sup> and chymotrypsin<sup>5</sup> (25 kDa).

### Conclusions

The main reasons for the use of non-soluble polyelectrolytes matrix are their adsorption capacities and the advantages of being non-expensive, easily available, and nontoxic. Previous reports have demonstrated the usefulness of the natural polyelectrolytes bed like Alg or chitosan as adsorbent of macromolecules. There are few studies about the molecular mechanism of interaction between the target enzymes, included in its natural biomass, with these beds. There is also poor information of the matrix behavior when it is working as a packed bed. In the present work, we have evaluated the capacity of cross-linked Alg-GG bed to interact with Try. These studies were performed in batch and in a packed bed column. Try was selected because of its well-known application in different biotechnological processes.

The first step to apply in the study of an adsorption process must be the determination of the adsorption isotherms to evaluate the adsorption capacity of the system. Our results showed for both working temperatures that the adsorption process has a sigmoid behavior consistent with the fact that the data fits the Hill model which indicates that the adsorption process induces a structural modification of the matrix.

Thermodynamic analysis of the data showed a positive  $\Delta H^\circ$  and  $\Delta S^\circ$ , indicating that the enzyme-matrix interaction occurs, mainly, by a disorder of the water structured around the polysaccharide chain of the bed. This finding agrees with the fact that the presence of a high NaCl concentration and polypropylene glycol is needed to induce the enzyme release from the matrix.

BDST model is based on the surface reaction rate theory. It gives an idea of the efficiency of the column under constant

operating conditions. The main design criterion is to predict how long the biosorbent will be able to sustain a specific amount of impurity from the solution before regeneration is needed. The breakthrough lines did not pass through origin which suggests that the adsorption mechanism in the fixed bed is not only because of a diffusion of the protein from the solution to the bed surface. However, the BDST model could be applied in a range of  $C/C_0$  ratio with low error as a simple model to predict the relationship between bed height ( $Z$ ) and service time ( $t$ ) in terms of process concentration and bioadsorption parameters.

The Alg-GG matrices proved to be an excellent protein adsorbent with the advantage to be eco-friendly and cost-efficient system.

### Acknowledgments

This research was supported by grants from FonCyT, Project PICT 2013-271 Argentina Innovator 2020. We thank Paola Camiscia for the language correction of the manuscript.

### Notation

Alg = alginate  
BDST = bed depth service time  
GG = guar gum  
Try = trypsin

### Literature Cited

- Kunitz M, Northrop JH. Crystalline chymo-trypsin and chymo-trypsinogen. I. Isolation, crystallization, and general properties of a new proteolytic enzyme and its precursor. *J Gen Physiol.* 1935;18(4):433-458.
- Guyonnet V, Thucik F, Long PL, Polanowski A, Travis J. Purification and partial characterization of the pancreatic proteolytic enzymes trypsin, chymotrypsin and elastase from the chicken. *J Chromatogr A.* 1999;852(1):217-225.
- Kumar M, Tamilarasan R, Sivakumar V. Adsorption of Victoria blue by carbon/Ba/alginate beads: kinetics, thermodynamics and isotherm studies. *Carbohydr Polym.* 2013;98(1):505-513.
- Roy I, Sardar M, Gupta MN. Cross-linked alginate-guar gum beads as fluidized bed affinity media for purification of jacalin. *Biochem Eng J.* 2005;23(3):193-198.
- Valetti NW, Picó G. Adsorption isotherms, kinetics and thermodynamic studies towards understanding the interaction between cross-linked alginate-guar gum matrix and chymotrypsin. *J Chromatogr B.* 2016;1012:204-210.
- Piyakulawat P, Praphairaksit N, Chantarasiri N, Muangsin N. Preparation and evaluation of chitosan/carrageenan beads for controlled release of sodium diclofenac. *AAPS PharmSciTech.* 2007; 8(4):120-130.
- Alvarez-Lorenzo C, Blanco-Fernandez B, Puga AM, Concheiro A. Crosslinked ionic polysaccharides for stimuli-sensitive drug delivery. *Adv Drug Deliv Rev.* 2013;65(9):1148-1171.
- Lee KY, Mooney DJ. Alginate: properties and biomedical applications. *Prog Polym Sci.* 2012;37(1):106-126.
- Spelzini D, Farruggia B, Picó G. Purification of chymotrypsin from pancreas homogenate by adsorption onto non-soluble alginate beads. *Process Biochem.* 2011;46(3):801-805.
- Gu F, Amsden B, Neufeld R. Sustained delivery of vascular endothelial growth factor with alginate beads. *J Controlled Release.* 2004;96(3):463-472.
- Brassesso ME, Valetti NW, Picó G. Molecular mechanism of lysozyme adsorption onto chemically modified alginate guar gum matrix. *Int J Biol Macromol.* 2017;96:111-117.



12. Yoon S-J, Chu D-C, Juneja LR. Chemical and physical properties, safety and application of partially hydrolyzed guar gum as dietary fiber. *J Clin Biochem Nutr.* 2008;42(1):1–7.
13. Gildberg A, Overbø K. Purification and characterization of pancreatic elastase from Atlantic cod (*Gadus morhua*). *Comp Biochem Physiol B Biochem Mol Biol.* 1990;97(4):775–782.
14. Foo KY, Hameed BH. Insights into the modeling of adsorption isotherm systems. *Chem Eng J.* 2010;156(1):2–10.
15. Günay A, Ersoy B, Dikmen S, Evcin A. Investigation of equilibrium, kinetic, thermodynamic and mechanism of Basic Blue 16 adsorption by montmorillonitic clay. *Adsorption.* 2013;19(2–4):757–768.
16. Valetti NW, Lombardi J, Boeris V, Picó G. Precipitation of chymotrypsin from fresh bovine pancreas using ι-carrageenan. *Process Biochem.* 2012;47(12):2570–2574.
17. Dotto G, Esquerdo V, Vieira M, Pinto L. Optimization and kinetic analysis of food dyes biosorption by *Spirulina platensis*. *Colloids Surf B Biointerfaces.* 2012;91:234–241.
18. Sathishkumar M, Binupriya AR, Vijayaraghavan K, Yun SI. Two and three-parameter isothermal modeling for liquid-phase sorption of Procion Blue H-B by inactive mycelial biomass of *Panus fulvus*. *J Chem Technol Biotechnol.* 2007;82(4):389–398.
19. Rangabhashiyam S, Anu N, Nandagopal MG, Selvaraju N. Relevance of isotherm models in biosorption of pollutants by agricultural byproducts. *J Environ Chem Eng.* 2014;2(1):398–414.
20. Wolman FJ, Copello GJ, Mebert AM, Targovnik AM, Miranda MV, Navarro del Cañizo AA, Díaz LE, Cascone O. Egg white lysozyme purification with a chitin–silica-based affinity chromatographic matrix. *Eur Food Res Technol.* 2010;231(2):181–188.
21. Aksu Z, Gönen F. Biosorption of phenol by immobilized activated sludge in a continuous packed bed: prediction of breakthrough curves. *Process Biochem.* 2004;39(5):599–613.
22. Jang J, Lee DS. Enhanced adsorption of cesium on PVA-alginate encapsulated Prussian blue-graphene oxide hydrogel beads in a fixed-bed column system. *Bioresour Technol.* 2016;218:294–300.
23. Zulfadhly Z, Mashitah M, Bhatia S. Heavy metals removal in fixed-bed column by the macro fungus *Pycnoporus sanguineus*. *Environ Pollut.* 2001;112(3):463–470.
24. Srivastava V, Prasad B, Mishra I, Mall I, Swamy M. Prediction of breakthrough curves for sorptive removal of phenol by bagasse fly ash packed bed. *Ind Eng Chem Res.* 2008;47(5):1603–1613.
25. Jain M, Garg V, Kadirvelu K. Cadmium (II) sorption and desorption in a fixed bed column using sunflower waste carbon calcium–alginate beads. *Bioresour Technol.* 2013;129:242–248.
26. Keller PJ, Cohen E, Neurath H. The proteins of bovine pancreatic juice. *J Biol Chem.* 1958;233(2):344–349.
27. Bukrinsky JT, Bjerrum MJ, Kadziola A. Native carboxypeptidase A in a new crystal environment reveals a different conformation of the important tyrosine 248. *Biochemistry.* 1998;37(47):16555–16564.

Manuscript received Mar. 9, 2018, and revision received Aug. 8, 2018.